Journal of Unmanned Vehicle Systems
Revue des systèmes de véhicules télécommandés

Object-based analysis of UAS imagery to map emergent and submerged invasive aquatic vegetation: a case study

Journal:	*Journal of Unmanned Vehicle Systems*
Manuscript ID	juvs-2016-0009.R1
Manuscript Type:	Note
Date Submitted by the Author:	23-Sep-2016
Complete List of Authors:	Chabot, Dominique; droneMetrics Dillon, Christopher; droneMetrics Ahmed, Oumer; Trent University, Geomatics, Remote Sensing and Land Resources Laboratory Shemrock, Adam; AirTech UAV Solutions
Keyword:	invasive species, OBIA, remote sensing, UAV, wetland monitoring

Object-based analysis of UAS imagery to map emergent and submerged invasive aquatic vegetation: a case study

Dominique Chabot[1], Christopher Dillon[1], Oumer Ahmed[2], and Adam Shemrock[3]

[1] droneMetrics, 7 Tauvette Street, Ottawa, Ontario, K1B 3A1, Canada

[2] Geomatics, Remote Sensing and Land Resources Laboratory, Trent University, 1600 West Bank Drive, Peterborough, Ontario, K9L 0G2, Canada

[3] AirTech UAV Solutions, 1071 Kam Avenue, Inverary, Ontario, K0H 1X0, Canada

Corresponding author: Dominique Chabot (e-mail: dominique.chabot@mail.mcgill.ca)

Abstract: Small unmanned aircraft systems (UAS) combined with automated image analysis may provide an efficient alternative or complement to labour-intensive boat-based monitoring of invasive aquatic vegetation. We trialled a small mapping drone for collecting high-resolution (≤5 cm/pixel) true-colour and near-infrared imagery revealing the distribution of invasive water soldier (*Stratiotes aloides*) in the Trent-Severn Waterway, Ontario (Canada). We further evaluated the capacity of an object-based image analysis approach based on the Random Forests classification algorithm to map features in the imagery, chiefly emergent and submerged water soldier colonies. The imagery contained flaws and inconsistencies resulting from data collection in suboptimal weather conditions that likely negatively impacted classification performance. Nevertheless, our best-performing classification had a producer's and user's accuracy for water soldier of 81% and 74%, respectively, an overall accuracy of 78%, and a kappa value of 61%, indicating "substantial" accuracy. This trial provides an instructive case study on results achieved in a "real-world" application of a UAS for environmental monitoring, notably characterized by time constraints for data collection and analysis. Beyond avoiding data collection in unfavourable weather conditions, adaptations of the image segmentation process and use of a true discrete-band multispectral camera may help to improve classification accuracy, particularly of submerged vegetation.

Key words: image classification, invasive species, OBIA, remote sensing, UAV, wetland monitoring

Introduction

Water soldier (*Stratiotes aloides*) is an aquatic plant native to Europe and northwest Asia that has become an invasive species of concern in the Trent River, Ontario (Canada), crowding out native vegetation, altering water chemistry, hindering recreational activities, and injuring people with its sharp serrated leaf edges (OFAH/OMNR 2012). The Ontario Ministry of Natural Resources and Forestry (OMNRF) in collaboration with various partnering agencies are engaged in a water soldier monitoring and control initiative focused on the Trent-Severn Waterway, testing solutions such as mechanical harvesting and herbicide to eliminate the plant. Continued monitoring of its extent and distribution is critical for appropriate application of control measures and assessment of their effectiveness. To date, monitoring has been accomplished by means of boat-based surveys, which are labour-intensive in the field. Consequently, a more convenient and efficient monitoring approach would be of interest, if suitably reliable and economical.

Small unmanned aircraft systems (UAS) have proven useful for very high-resolution (<10 cm/pixel) aerial surveys of areas and habitats that are challenging to access or navigate at ground level, notably wetland (Madden et al. 2015), riverine (Birdsong et al. 2015) and aquatic environments in general (Husson et al. 2014; DeBell et al. 2016; Turner et al. 2016). Moreover, efforts have been invested in developing approaches to automate habitat, vegetation or land cover classification in the uniquely high-resolution imagery collected by UAS, including several studies focused on wetland and aquatic vegetation (Goktogan et al. 2010; Zaman et al. 2011; Lechner et al. 2012; Chabot and Bird 2013; Kalacska et al. 2013; Knoth et al. 2013; Flynn and Chapra 2014; Casado et al. 2015; Zweig et al. 2015). It has been noted that the fine-scale spectral heterogeneity resulting from the very high resolution of UAS imagery tends to make it challenging to classify using traditional pixel-based spectral classification methods, and consequently object-based image analysis (OBIA) has been advocated as a more effective approach to classification (Whitehead and Hugenholtz 2014).

The aim of this trial study was to evaluate the effectiveness of UAS-based monitoring of water soldier encroachment on the Trent-Severn Waterway, and specifically the capacity to automate detection and mapping of emergent and submerged colonies in UAS imagery using OBIA classification methods. A further purpose of this note is to provide an example of a "real-world" application of a UAS for environmental monitoring and the results thereof, characterized by time constraints, suboptimal weather conditions during data collection, and an overall prioritization of efficiency over thoroughness.

Materials and methods

Study area

The trial focused on a ~50-ha shallow-water (mostly <1 m) bay (44.377˚N, 77.828˚W) in the Trent River (Fig. 1). Native aquatic vegetation occurring in the bay includes tapegrasses (Hydrocharitaceae family), water/pond lilies (Nymphaeaceae family), slender naiad (*Najas flexilis*), floating-leaf pondweed (*Potamogeton natans*), water crowfoot (Ranunculus family), coontail (*Ceratophyllum demersum*), stoneworts (Characeae family), and bulrush (*Scirpus* spp.). The bay and surrounding water bodies have been the focus of experimental water soldier control treatments, and a coarse-scale map of water soldier distribution in the general area was produced in 2015 (Fig. 1) by sampling the presence/absence and abundance of water soldier from a boat throughout a 50 x 50-m grid.

Data collection

We collected aerial imagery with an eBee "mapping drone" (senseFly, Cheseaux-Lausanne, Switzerland), an ~700-g UAS featuring a foam delta-winged airframe of ~1-m wingspan. Flights over the study area were conducted during the morning of 15 October 2015. Sky conditions were partly cloudy with winds ~30 km/h gusting to ~40 km/h. Two flights were completed at an altitude of 137 m (450 ft) AGL to collect true-colour (RGB) and near-infrared (NIR) imagery. RGB imagery was acquired with an 18.2-megapixel Sony Cyber-shot DSC-WX220, yielding a ground sample distance (GSD) of 3.9 cm/pixel. NIR imagery was acquired with a 12-megapixel Canon PowerShot S110 modified to capture NIR, yielding a GSD of 5.4 cm/pixel. Each camera captured 253 photos with 70% forward and lateral overlap. We then post-processed photos into orthomosaics using Postflight Terra 3D v4.0 (senseFly). Georeferencing was based on the aircraft's GPS data in combination with data recorded by the autopilot's inertial measurement unit to correct for angular offsets. We subsequently re-referenced the NIR imagery directly to the RGB imagery to improve the alignment of the orthomosaics ahead of their combined use in OBIA.

Additionally, ground truthing was carried out in the bay on 2 November 2015 to provide image classification training data. A series of GIS polygons were first drawn around clearly discernible submerged and emergent vegetation colonies in the RGB orthomosaic, to which surveyors then navigated by boat and recorded the dominant vegetation type. A total of 92 samples were collected in this manner.

Image classification

Following the OBIA approach, we first performed multi-resolution image segmentation using the ENVI v5.1 (Exelis, Boulder, CO, USA) Feature Extraction module on a combination of the RGB bands and the NIR band, with a scale level of 78 and merge level of 95, resulting in 100,433 image objects of varying size and shape throughout the area of the bay. We then classified the segmented objects using the Random Forests (RF) algorithm (Breiman 2001), a "machine learning" approach to image classification based on inputting training samples, as opposed to manually developing an object classification rule set. RF is known to be particularly efficient when dealing with large numbers of input variables, and has previously been employed to classify high-resolution UAS imagery (Kelcey and Lucieer 2013; Feng et al. 2015; Ma et al. 2015; Gonçalves et al. 2016). Since the ground-truth samples were often clustered and not distributed throughout the study area, we merely used them to initially develop familiarity with the appearance of various vegetation types in the imagery. We then selected representative training samples (i.e. image objects) throughout the study area based on visual interpretation of the imagery (Chabot and Bird 2013; Zweig et al. 2015), defining the following four classes: (1) emergent water soldier; (2) submerged water soldier; (3) native vegetation; (4) other. In an effort to evaluate whether the number of inputted training samples affects classification accuracy, we performed a classification based on 130 training samples (minimum of 30 per class) as well as a classification based on half of the training samples (65), selected at random.

Classification assessment

We evaluated classification accuracy by generating 400 randomly placed points throughout the imagery, which we manually classified based on visual interpretation and in turn compared to the automated RF classifications. For both RF classifications (65 and 130 training samples), we constructed a confusion matrix in relation to the manual classification and calculated standard accuracy metrics, namely the producer's accuracy (PA), the user's accuracy (UA), the overall accuracy (OA), and the kappa statistic.

Results

The overall highest accuracy was achieved in the RF classification based on 65 training samples, and a side-by-side comparison of this classified image of the study area to a composite image of the raw RGB and NIR bands is shown in Fig. 2. The overall accuracy (73.50%) and kappa value (55.23%) of the 65-training-sample classification (Table 1) were marginally higher than those of the 130-training-sample classification (OA = 69.50%, kappa = 47.15%) (Table 2). According to Sim and Wright (2005), these kappa values are indicative of "moderate" agreement (≤0% = poor; 1–20% = slight; 21–40% = fair; 41–60% = moderate; 61–80% = substantial; 81–100% = almost perfect). The superior performance of the former classification was mainly driven by more accurate classification of submerged water soldier, although overall both classifications struggled with this class compared to the others (Tables 1, 2). Both classifications also undermapped native vegetation (PA = 35.29–36.76%), although points classified as such were mostly correct (UA = 78.13–82.76%).

Since submerged and emergent water soldier tended to be misclassified as one another, merging these two classes in the 65-training-sample classification (Table 3) resulted in a higher accuracy for the unified water soldier class (PA = 81.13%, UA = 74.14%) than either the submerged or emergent class when considered separately, as well as a higher overall accuracy (78.25%) and kappa value (60.62%), just about crossing the threshold to "substantial" agreement.

Discussion

Overall, the eBee UAS combined with the RF/OBIA classification approach proved promising for mapping invasive water soldier, although it is likely that the particularly windy conditions during data collection negatively affected image classification performance in this trial. Close examination of the imagery revealed variation in water surface perturbation throughout the orthomosaics—ranging from calm to light ripples, waves and white caps—that may have hindered classification of submerged vegetation. Furthermore, certain portions of the imagery were blurrier, likely the result of photos being captured as the lightweight aircraft was being jostled by gusts. This would tend to distort image texture information used by the classification algorithm. Whereas most previous studies involving classification of aquatic vegetation in UAS imagery—some reporting overall accuracies ≥90% and kappa values ≥80%—were carried out in the context of academic research where there is generally more flexibility to plan for data collection under ideal conditions, our trial provides an instructive case study on the potential consequences of more urgent data collection in the context of a work contract where there was concern over the dwindling vegetation season.

A compounding challenge we faced was that of performing a single classification across our entire relatively large image set (only cropping out areas outside the bay itself), in contrast to several previous studies that either only classified a small portion of the collected imagery and/or divided imagery into multiple subsets, each subject to an independent classification that limited the degree of imagery variation encountered by any individual classification (Lechner et al. 2012; Chabot and Bird 2013; Kalacska et al. 2013). Also, few studies have specifically involved automated classification of submerged vegetation in UAS imagery. Casado et al. (2015) similarly struggled to classify submerged vegetation, with a producer's accuracy of 29% despite an overall classification accuracy of 81%. Flynn and Chapra (2014) achieved a classification accuracy of 92%

for submerged *Cladophora* along a 1-km stretch of a shallow non-turbid river, although the river was virtually devoid of any other types of vegetation, and thus only two classes were defined: "*Cladophora*" and "background".

Another apparent cause of poor classification accuracy for submerged water soldier was under-segmentation of deeper water areas containing submerged vegetation compared to areas of emergent vegetation, likely resulting from the dampened spectral contrasts and saturation of submerged features to which the segmentation process was not as sensitive. A potential workaround without in turn over-segmenting areas of emergent vegetation might be to perform an additional hierarchically "nested" segmentation (Benz et al. 2004) of objects in deeper areas only, then re-merge these with the rest of the objects from the initial segmentation. Imagery collected with a true discrete-band multispectral camera may also yield better vegetation segmentation and classification results. More sophisticated analytical methods of deriving submerged vegetation depth and properties from low-altitude optical imagery have been demonstrated (Visser et al. 2015), but employing these would ultimately significantly reduce the efficiency of UAS-based water soldier monitoring compared to traditional boat-based surveys.

The fact that the 130-training-sample classification did not outperform the 65-training-sample classification seems to suggest that only a modest number of training samples may be required to achieve an optimal RF classification, so long as they collectively capture a sufficient amount of intra- and inter-class variation. However, more rigorous testing is required to substantiate this conclusion, for example repeatedly running the RF algorithm on different randomly selected subsets of training samples, and experimenting with different numbers of trees and/or depths in the algorithm parameters. Due to the expeditious nature of this trial, expanded testing of this sort was beyond the scope of our objectives. Finally, although it is convenient that

UAS imagery classification is not as reliant on ground truthing as coarser-resolution traditional aerial imagery, it may always be desirable to collect at least some ground data to help familiarize the interpreter with the appearance of different feature classes in the imagery and provide definitive validation of classification results.

Acknowledgements

This trial was conceived, designed and funded by the Aviation, Forest Fire and Emergency Services (AFFES) of the Ontario Ministry of Natural Resources and Forestry. We thank C. Sallaway (OMNRF), A. Brunet (AFFES – OMNRF) and the Ontario Federation of Anglers and Hunters for collecting the ground truth data, as well as the owners of the land adjacent to the study area for allowing us to deploy the UAS from their property. UAS flights were authorized by a Special Flight Operations Certificate (ATS-15-16-00043103) issued by Transport Canada.

References

Benz, U.C., Hofmann, P., Willhauck, G., Lingenfelder, I., and Haynen, M. 2004. Multi-resolution, object-oriented fuzzy analysis of remote sensing data for GIS-ready information. ISPRS Journal of Photogrammetry and Remote Sensing. **58**: 239–258.

Birdsong, T.W., Bean, M., Grabowski, T.B., Hardy, T.B., Heard, T., Holdstock, D., Kollaus, K., Magnelia, S., and Tolman, K. 2015. Application and utility of a low-cost unmanned aerial system to manage and conserve aquatic resources in four Texas rivers. Journal of the Southeastern Association of Fish and Wildlife Agencies. **2**: 80–85.

Breiman, L. 2001. Random Forests. Machine Learning. **45**: 5–32.

Casado, M.R., Gonzalez, R.B., Kriechbaumer, T., and Veal, A. 2015. Automated identification of river hydromorphological features using UAV high resolution aerial imagery. Sensors. **15**: 27969–27989.

Chabot, D., and Bird, D.M. 2013. Small unmanned aircraft: precise and convenient new tools for surveying wetlands. Journal of Unmanned Vehicle Systems. **1**: 15–24.

DeBell, L., Anderson, K., Brazier, R.E., King, N., and Jones, L. 2016. Water resource management at catchment scales using lightweight UAVs: current capabilities and future perspectives. Journal of Unmanned Vehicle Systems. **4**: 7–30.

Feng, Q., Liu, J., and Gong, J. 2015. UAV remote sensing for urban vegetation mapping using Random Forest and texture analysis. Remote Sensing. **7**: 1074–1094.

Flynn, K.F., and Chapra, S.C. 2014. Remote sensing of submerged aquatic vegetation in a shallow non-turbid river using an unmanned aerial vehicle. Remote Sensing. **6**: 12815–12836.

Goktogan, A.H., Sukkarieh, S., Bryson, M., Randle, J., Lupton, T., and Hung, C. 2010. A rotary-wing unmanned air vehicle for aquatic weed surveillance and management. Journal of Intelligent and Robotic Systems. **57**: 467–484.

Gonçalves, J., Henriques, R., Alves, P., Sousa-Silva, R., Monteiro, A.T., Lomba, A., Marcos, B., and Honrado, J. 2016. Evaluating an unmanned aerial vehicle-based approach for assessing habitat extent and condition in fine-scale early successional mountain mosaics. Applied Vegetation Science. **19**: 132–146.

Husson, E., Hagner, O., and Ecke, F. 2014. Unmanned aircraft systems help to map aquatic vegetation. Applied Vegetation Science. **17**: 567–577.

Kalacska, M., Arroyo-Mora, J.P., de Gea, J., Snirer, E., Herzog, C., and Moore, T.R. 2013. Videographic analysis of *Eriophorum vaginatum* spatial coverage in an ombotrophic bog. Remote Sensing. **5**: 6501–6512.

Kelcey, J., and Lucieer, A. 2013. An adaptive texture selection framework for ultra-high resolution UAV imagery. Proceedings of the IEEE International Geoscience and Remote Sensing Symposium, 21–26 July 2013, Melbourne, Australia. pp. 3883–3886.

Knoth, C., Klein, B., Prinz, T., and Kleinebecker, T. 2013. Unmanned aerial vehicles as innovative remote sensing platforms for high-resolution infrared imagery to support restoration monitoring in cut-over bogs. Applied Vegetation Science. **16**: 509–517.

Lechner, A.M., Fletcher, A., Johansen, K., and Erskine, P. 2012. Characterising upland swamps using object-based classification methods and hyper-spatial resolution imagery derived from an unmanned aerial vehicle. ISPRS Annals of the Photogrammetry, Remote Sensing and Spatial Information Sciences. **I-4**: 101–106.

Ma, L., Cheng, L., Li, M., Liu, Y., and Ma, X. 2015. Training set size, scale, and features in geographic object-based image analysis of very high resolution unmanned aerial vehicle imagery. ISPRS Journal of Photogrammetry and Remote Sensing. **102**: 14–27.

Madden, M., Jordan, T., Bernades, S., Cotten, D.L., O'Hare, N., and Pasqua, A. 2015. Unmanned aerial systems and structure from motion revolutionize wetlands mapping. *In* Remote Sensing of Wetlands: Applications and Advances. *Edited by* R.W. Tiner, M.W. Lang, and V.V. Klemas. CRC Press/Taylor & Francis Group, Boca Raton, FL, USA. pp. 195–219.

OFAH/OMNR (Ontario Federation of Anglers and Hunters/Ontario Ministry of Natural Resources). 2012. Water soldier. Invading Species Awareness Program. *Retrieved online from*: http://www.invadingspecies.com/invaders/plants-aquatic/water-soldier/

Sim, J., and Wright, C.C. 2005. The kappa statistic in reliability studies: use, interpretation, and sample size requirements. Physical Therapy. **85**: 257–268.

Turner, I.L., Harley, M.D., and Drummond, C.D. 2016. UAVs for coastal surveying. Coastal Engineering. **114**: 19–24.

Visser, F., Buis, K., Verschoren, V., and Meire, P. 2015. Depth estimation of submerged aquatic vegetation in clear water streams using low-altitude optical remote sensing. Sensors. **15**: 25287–25312.

Whitehead, K., and Hugenholtz, C.H. 2014. Remote sensing of the environment with small unmanned aircraft systems (UASs), part 1: a review of progress and challenges. Journal of Unmanned Vehicle Systems. **2**: 69–85

Zaman, B., Jensen, A.M., and McKee, M. 2011. Use of high-resolution multispectral imagery acquired with an autonomous unmanned aerial vehicle to quantify the spread of an invasive wetland species. Proceedings of the IEEE International Geoscience and Remote Sensing Symposium, 24–29 July 2011, Vancouver, Canada. pp. 803–806.

Zweig, C.L., Burgess, M.A., Percival, H.F., and Kitchens, W.M. 2015. Use of unmanned aircraft systems to delineate fine-scale wetland vegetation communities. Wetlands. **35**: 303–309.

Table 1. Confusion matrix of the 65-training-sample automated classification of UAS imagery (rows) in relation to manual interpretation of the imagery (columns) for mapping invasive emergent and submerged water soldier in the Trent-Severn Waterway, Ontario (Canada).

	Em. water soldier	Sub. water soldier	Native vegetation	Other	Total	User's accuracy	Commission error
Em. water soldier	38	9	3	4	54	70.37%	29.63%
Sub. water soldier	10	29	10	13	62	46.77%	53.23%
Native vegetation	0	0	25	7	32	78.13%	21.87%
Other	4	16	30	202	252	80.16%	19.84%
Total	52	54	68	226	400		
Producer's accuracy	73.08%	53.70%	36.76%	89.38%		**Overall accuracy**	**73.50%**
Omission error	26.92%	46.30%	63.24%	10.62%		**Kappa**	**55.23%**

Table 2. Confusion matrix of the 130-training-sample automated classification of UAS imagery (rows) in relation to manual interpretation of the imagery (columns) for mapping invasive emergent and submerged water soldier in the Trent-Severn Waterway, Ontario (Canada).

	Em. water soldier	Sub. water soldier	Native vegetation	Other	Total	User's accuracy	Commission error
Em. water soldier	34	7	2	3	46	73.91%	26.09%
Sub. water soldier	14	18	11	16	59	30.51%	69.49%
Native vegetation	0	0	24	5	29	82.76%	17.24%
Other	4	29	31	202	266	75.94%	24.06%
Total	52	54	68	226	400		
Producer's accuracy	65.38%	33.33%	35.29%	89.38%		**Overall accuracy**	**69.50%**
Omission error	34.62%	66.67%	64.71%	10.62%		**Kappa**	**47.15%**

Table 3. Confusion matrix of the 65-training-sample automated classification of UAS imagery (rows) in relation to manual interpretation of the imagery (columns) for mapping invasive water soldier (with emergent and submerged classes merged) in the Trent-Severn Waterway, Ontario (Canada).

	Water soldier	Native vegetation	Other	Total	User's accuracy	Commission error
Water soldier	86	13	17	116	74.14%	25.86%
Native vegetation	0	25	7	32	78.13%	21.87%
Other	20	30	202	252	80.16%	19.84%
Total	106	68	226	400		
Producer's accuracy	81.13%	36.76%	89.38%		**Overall accuracy**	**78.25%**
Omission error	18.87%	63.24%	10.62%		**Kappa**	**60.62%**

Fig. 1. Map of invasive water soldier distribution in 2015 in the Lake Seymour area, Ontario (Canada), estimated by means of boat-based surveys (produced by the Ontario Ministry of Natural Resources and Forestry; © Queen's Printer for Ontario 2015). Red zones = dense colonies; beige zones = scattered plants; yellow zones = single plants; black rectangle = study area where UAS aerial imagery was collected.

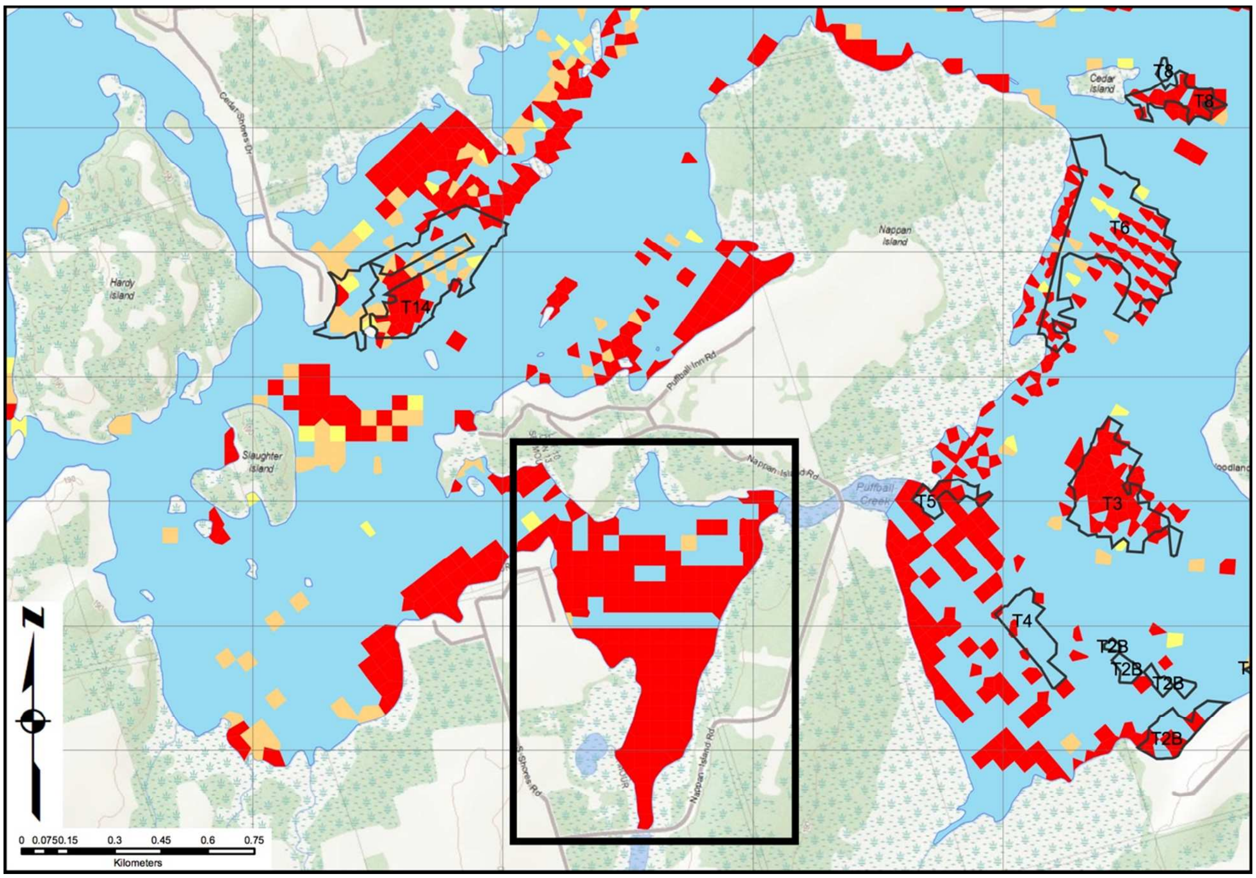

Fig. 2. Composite true-colour and near-infrared UAS imagery (left) of the bay study area in the Trent-Severn Waterway, Ontario (Canada), and 65-training-sample classified image (right). Red zones = emergent water soldier; beige zones = submerged water soldier; green zones = native vegetation, blue zones = other.